ChemPubSoc Europe

DOI: 10.1002/cptc.201800068

CHEMPHOTOCHEM Communications

Special Issue

One-Pot Synthesis of Diverse γ-Lactam Scaffolds Facilitated by a Nebulizer-Based Continuous Flow Photoreactor

Georgios I. Ioannou,[a] Tamsyn Montagnon,[a] Dimitris Kalaitzakis,[a] Spiros A. Pergantis,[a] and Georgios Vassilikogiannakis*[a]

The use of a modified prototype continuous flow reactor (CFR) as a pivotal part of a number of versatile singlet oxygen-mediated reaction sequences is presented herein. These sequences target rapid access to structural complexity and diversity. The prototype reactor achieves high conversions and productivities by attaining large specific surface areas for these biphasic reactions. In the reactor, the reaction solution is nebulized (using either oxygen or air) and the resulting aerosol is irradiated by an LED jacket that surrounds the Pyrex reaction chamber. The one pot procedures developed herein are, according to many different criteria, both highly efficient and green. The key common intermediates and the source of both the complexity and variety of the final products are *N*-acyl imminium ions (NAI; protonated *N*-acyl enamines). The initial substrates are simple and readily accessible furans and the diverse array of products is composed of different complex γ-lactams. Many of the products are of particular interest due to their close relationships to known biologically active molecules.

The concept of ideal synthesis,[1] which was upgraded and further developed a few years ago,[2] probably sets out the most comprehensive picture of the challenges modern organic synthesis is embracing. Yet, this concept is far from simple when it comes to the implementation because it encompasses so many diverse factors all contributing equally to the whole. As a result, many efforts have focused on fine tuning a small number of aspects rather than taking on the complete fully-integrated paradigm. In our own work, we have regularly explored, either independently or in small packages, such themes (use of benign reagents & atom-economy especially for oxidations, step-economy achieved by bundling transformations together into one pot operations and rapid access to structural diversity through repeated manipulation of key intermediates bearing multiple reactive sites).[3] In the current investigation, an attempt has been made to expand the remit to achieve a more advanced combination which includes newly developed atom- & step-economic transformations alongside facilitated scale-up using a modified prototype continuous flow system.

In this work, the reactive intermediate targeted as a highly flexible source of structural diversity is the *N*-acyl imminium ion (NAI), formed upon protonation of an *N*-acyl enamine (**2**; Scheme 1). NAIs have long been appreciated and have been

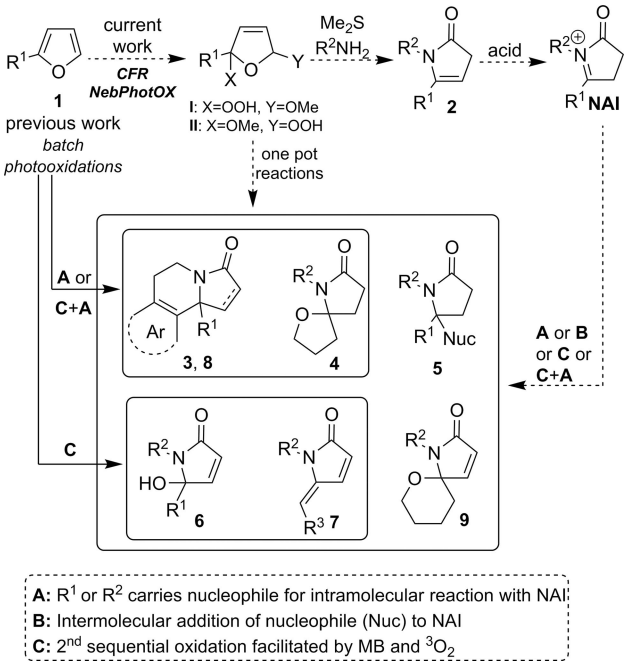

Scheme 1. Rapid and scalable access to a diverse array of γ-lactams.

widely employed in a broad range of synthetic methodologies.[4,5] We have, however, developed a unique way of making them in situ as part of one pot batch reaction sequences which have many inherent advantages over more traditional approaches.[6] These sequences are highly atom-economic and use singlet oxygen ($^1O_2$) as a selective, clean and waste-free facilitator/oxidant. The initial substrates are readily accessible (incl. from biomass) furans whose substitution patterns are relatively trivial to manipulate as desired. The sequences oversee rapid and dramatic increases in molecular complexity, minimize solvent use and avoid unnecessary purifications; furthermore, they exhibit high overall yields.

[a] Dr. G. I. Ioannou, Dr. T. Montagnon, Dr. D. Kalaitzakis, Prof.Dr. S. A. Pergantis, Prof. Dr. G. Vassilikogiannakis
Department of Chemistry
University of Crete
Vasilika Vouton, 71003, Crete (Greece)
E-mail: vasil@uoc.gr

Supporting information for this article is available on the WWW under https://doi.org/10.1002/cptc.201800068

An invited contribution to a Special Issue on Flow Photochemistry

Herein, for the first time in these $^1O_2$-sequences, intermolecular reactions between a number of electron-rich aromatic partners and the NAI intermediates are reported; thus, further expanding their scope. In addition, these methodologies would have been of little use if they could not have been effectively scaled-up, this important criteria has also been met for the first time for these sequences using a continuous flow reactor (CFR; Figure 1)[7] which ameliorates many of the hurdles traditionally

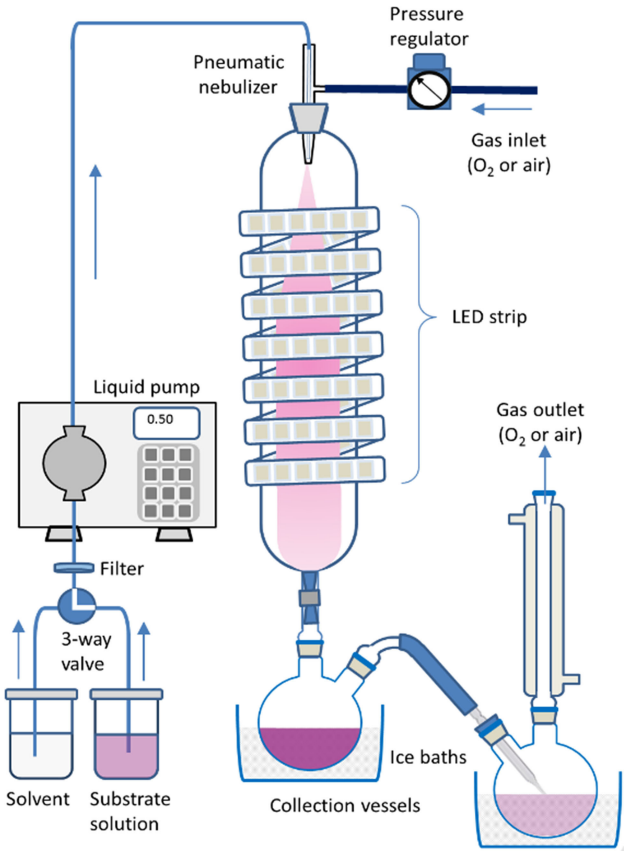

Figure 1. Schematic representation of the NebPhotOX continuous flow reactor set-up.

encountered when seeking to scale-up biphasic photochemical reactions. The overall outcome is that we are able to present herein a facile and scalable access to a diverse range of γ-lactam frameworks using clean and efficient chemistry.

To begin with, the modified reactor design will be presented and then there will be a discussion of the reaction sequences explored using this set-up. Continuous flow photochemistry, as this special issue attests to, is currently a highly productive and burgeoning area.[8] Those looking for novel ways to utilize singlet oxygen[9] have not remained immune to these rapidly evolving developments and as a result a variety of reactor types have been investigated encompassing both micro- and macroreactor engineering concepts.[7–10] In this field, there are two significant hurdles to overcome when developing a new technology. Firstly, the rapid attenuation of light as it travels through solutions (defined by the Bouger–Lambert–Beer law) causes light penetration issues as reactor scale increases. Secondly, the poor solubility of oxygen in reaction solvents imposes limitations on the reactor designs. Perhaps, the most frequently and easily employed solution to circumvent this latter issue is the use of segmented flow (also called Taylor or slug flow) wherein the substrate solution is interspersed with bubbles of gas at regular intervals increasing the gas-liquid interface area.[11,12] It should be noted that the light penetration challenge applies more generally to all photochemical reactions, and, therefore, has had a greater overall impact. To solve these problems both the surface area of the reaction solution that is exposed to light and the gas-liquid interface surface area should be maximized. Examples of how one, or sometimes both, these surface areas have been maximized include; using lengths of flexible tubing wrapped around the light source[13] (fluorinated ethylene propylene-FEP tubing,[10i–k] perfluoroalkoxy-PFA tubing,[10b,f,h] microcapilliary,[10b,f,h,j] parallel systems[10f,j]), thin-walled annular vessels,[10l] falling films,[10a] thin film,[10g] gas-liquid membranes,[10d] vortexes[10e] or mesofluidic devices.[10c] In our system (Figure 1), very high specific surface areas (conservatively estimated to be in the range of 100,000 to 1,000,000 m^2m^{-3}[7a,14]) have been attained by nebulizing the reaction solution. On generating such a fine aerosol both the gas-liquid interface and the surface area exposed to light are maximized.[15]

In more detail, in our CFR (NebPhotOX) a robust SeaSpray U-series nebulizer (that has a higher tolerance for dissolved solids than other comparable nebulizer heads) is supplied with the reaction solution (furan substrate and very low quantities of photosensitiser in methanol[16]) by a single piston liquid pump (actual flow rate of between 0.50–0.85 mL min^{-1}) and a nebulizing gas (oxygen or air).[17] The nebulizer discharges a fine aerosol into a cylindrical Pyrex chamber at atmospheric pressure and room temperature. During its passage through the chamber the aerosol is irradiated by an LED light jacket which surrounds the chamber.[18] During the current investigation, it was found that both the conversion and the final isolated yield could in some cases be improved if the chamber was secured upright (vertical) rather than angled horizontally (see below). This may maximize the lifetime of the nebula as the time before it interacts with the glass wall of the chamber is on average prolonged, as well as, aiding efficient collection. Notably, this CFR system has been constructed from relatively inexpensive and commercially available components. For example, a wide preparative glass chromatography column, which every synthetic laboratory has, can be used as the reaction chamber. With regard to the safety of this reactor design, the following should be considered. Firstly, the reaction chamber, which is not pressurized, has a volume of approximately 1.2 L, the gas flow used is 0.9 L min^{-1} and the solution flow is around 0.6 mL min^{-1} meaning that at any given moment the reaction chamber contains a small quantity (<1 mL) of nebulized methanolic solution which is combustible. In addition, as detailed in the Supporting Information, measures are taken to eliminate all possible ignition sources from the fumehood area. Adequate ventilation is also used to prevent stagnation of O_2 when used as nebulizing gas. With respect to

the peroxides formed as intermediates in the reaction sequences, only very small quantities are formed at any given time (especially, in comparison to equivalent batch reactions but even compared to other CFR systems), and, furthermore, these peroxides are rapidly reduced within the collection flask that is pre-charged (for large scale experiments) with dimethylsulfide. Again, in the equivalent batch reactions, reduction would not occur so rapidly and accumulation of larger quantities of peroxides over longer periods is normal. In this context, the Sanofi method for the industrial production of artemisinin employs a singlet oxygen-initiated cascade.[19] The reaction sequence takes place in large batch reactors (batch size ≈370 kg of isolated artemisinin) with both an oxygen source (air) and peroxide formation, neither of which were considered insurmountable hurdles when developing this industrial process technology.

Moving on to discuss the reaction sequences that were successfully conducted using the NebPhotOX system, the first examples investigated (reaction sequences of type A, Scheme 1) all contrived to place an internal nucleophile within the NAI intermediate that would then react intramolecularly. The results are presented in Table 1 (**1**→**3** or **4**). It should be noted that these sequences are very simple operations with the first step taking place in the CFR (0.5 M concentration for furans **1**) and all remaining transformations occurring in one pot, after the solutions from the two collection flasks had been combined. The source of the nucleophile was either the amine (**10**), added after the photooxidation and used to form the NAI intermediate[6] (Table 1, entries a and b, R^2 contains the nucleophile), or the initial furan substrate (**1c**, Table 1, R^1 bears a nucleophilic moiety). Notably, entry a also constitutes a total synthesis of the natural product glochidine (**3a**).[20] Both aforementioned scenarios were highly effective (with productivities[21] ranging from 0.23–0.31 mmol min^{-1}). Entry c also shows a direct comparison between the CFR system with the Pyrex chamber angled horizontally or fixed in a vertical position; it can be seen that the latter arrangement improves the conversion (92 vs 85%) at even higher flow rates (0.68 vs 0.55 mL min^{-1}), and, thus, the productivity (0.31 vs 0.23 mmol min^{-1}), but it also gives a better isolated yield (63 vs 56%). The flow rates entered in Tables 1–3 represent the actual flow rate which was measured and recorded for each experiment individually. Considering the number of discrete transformations (4 in total) included in these packaged reaction sequences, the overall yields are exceptionally high (they represent >84% for each discrete step).

Table 1. Results for reaction sequence of type A (either R^1 or R^2 contains a pendant nucleophile that reacts with the intermediate NAI).

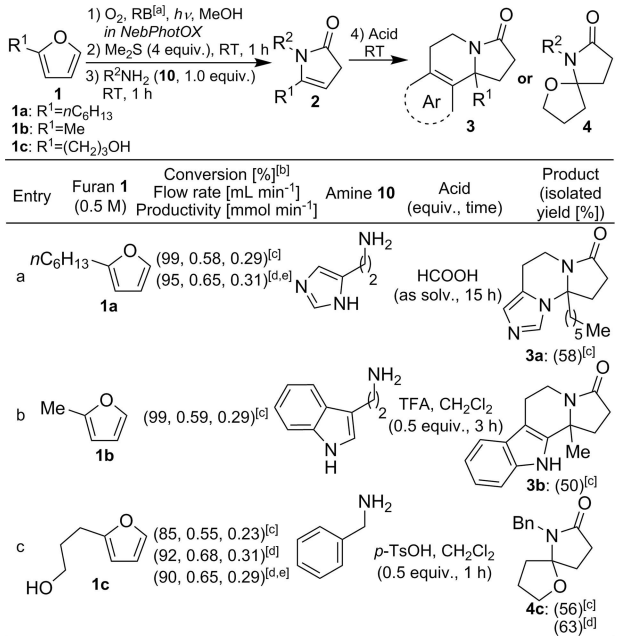

[a] 0.5 mol% of rose Bengal was used; [b] Conversions were determined by ^{1}H NMR of the crude mixtures; [c] Cyclindrical pyrex chamber employed horizontally in CFR set-up; [d] Cyclindrical pyrex chamber employed vertically in CFR set-up; [e] Nebulizing gas was air.

Intriguingly, when the oxygen was replaced with air as the nebulizing gas no significant reduction in conversion/productivity was seen (Table 1, entry c - conversion dropped only very marginally from 92 to 90%, on going from oxygen to air).

Next, the investigation proceeded by moving on to explore a set of more challenging intermolecular reactions (reaction sequences of type B, Scheme 1).[5] In this case, the NAI intermediate would react with an external electron rich aromatic partner (**11**, Table 2). Crucially, the intermolecular reaction yields a new quaternary carbon center in the expected products **5**. These intermolecular reactions have not previously been investigated in singlet oxygen-initiated reaction sequences. Gratifyingly and despite the additional hindrances in place here, the reactions proceeded smoothly; with the results being presented in Table 2. The productivities of the CFR (0.27–0.41 mmol min^{-1}) are high and the final isolated yields (51–66%) are remarkable given the complexity of the packages being tested. The importance of changing from a horizontally angled chamber set-up to having the chamber fixed vertically is seen in the significant improvements to the isolated yield (Table 2, entries d and g, 66 vs 56% and 62 vs 53%, respectively) and the productivities of NebPhotOX. When the nebulizing gas was changed from oxygen to air, a minor reduction in the conversion and isolated yield was seen (Table 2, entry d). This minor reduction is reasonable if we take into account that the molar ratio of O_2 vs furan drops by a factor of 5 on going from O_2 to air.

Following the success of the intermolecular reaction sequences, we next sought to add a second oxidation step to the reaction sequences (reaction sequences of type C, Scheme 1). This unique second oxidation, facilitated by methylene blue and this time using ground state oxygen ($^3O_2$),[6b,22] is beneficial as it can be used to introduce further functionality (such as, an extra degree of unsaturation) to the products; thus, enhancing their range and potential utility. The results are presented in Table 3 (**1**→**6**–**9**). It can be seen that the products of these reaction sequences bear multiple handles through which further manipulations could be orchestrated. In entries h and i, the products (**6h** and **7i**) contain a masked NAI

Table 2. Results for reaction sequence of type B (intermolecular reaction between electron rich aromatic compound and the NAI).

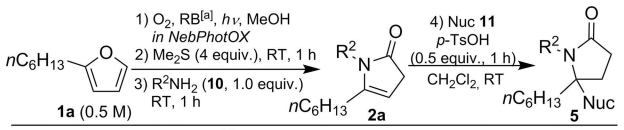

Entry	Conversion [%][b] Flow rate [mL min^{-1}] Productivity [mmol min^{-1}]	Amine 10	Nucleophile 11 (equiv.)	Product (isolated yield [%])
d	(99, 0.57, 0.28)[c] (99, 0.75, 0.37)[d] (92, 0.59, 0.27)[d,e]	$BnNH_2$	(1 equiv.)	**5d**: (56)[c] (66)[d] (51)[d,e]
e	(99, 0.58, 0.29)[c]	$BnNH_2$	(1 equiv.)	**5e**: (55)[c]
f	(99, 0.57, 0.28)[c]	NH_3	(1 equiv.)	**5f**: (51)[c]
g	(99, 0.58, 0.29)[c] (99, 0.83, 0.41)[d]	$MeNH_2$	(2 equiv.)	**5g**: (53)[c] (62)[d]

[a] 0.5 mol% of rose Bengal was used; [b] Conversions were determined by ^{1}H NMR of the crude mixtures; [c] Cyclindrical pyrex chamber employed horizontally in CFR set-up; [d] Cyclindrical pyrex chamber employed vertically in CFR set-up; [e] Nebulizing gas was air.

Table 3. Results for reaction sequence of type C (the sequence includes a second late-stage oxidation mediated by the photosensitiser methylene blue and $^3O_2$).

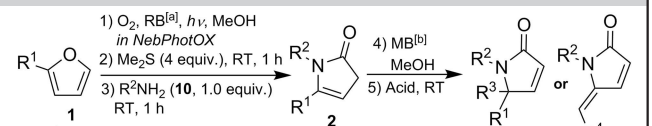

Entry	Furan 1 (0.5 M)	Conversion [%][c] Flow rate [mL min^{-1}] Productivity [mmol min^{-1}]	Amine 10	Acid (equiv., time)	Product (isolated yield [%])
h	1a	(99, 0.52, 0.26)[d] (99, 0.77, 0.38)[e] (90, 0.60, 0.27)[e,f]		–	**6h**: (62)[d] (59)[e] (50)[e,f]
i	1a	(99, 0.58, 0.29)[d]		*p*-TsOH, CH_2Cl_2 (1.0 equiv., 1 h)	**7i**: (58)[d]
j	1a	(99, 0.58, 0.29)[d]	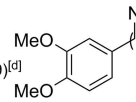	HCOOH (as solv., 1 h)	**8j**: (66)[d]
k	1d	(85, 0.54, 0.23)[d] (95, 0.74, 0.35)[e] (82, 0.63, 0.26)[e,f]	$MeNH_2$	*p*-TsOH, CH_2Cl_2 (0.5 equiv., 1 h)	**9k**: (58)[d] (53)[e] (49)[e,f]

[a] 0.5 mol% of rose Bengal was used; [b] 3 mol% of methylene blue was used; [c] Conversions were determined by ^{1}H NMR of the crude mixtures; [d] Cyclindrical pyrex chamber employed horizontally in CFR set-up; [e] Cyclindrical pyrex chamber employed vertically in CFR set-up; [f] Nebulizing gas was air.

which can be revealed if further reactions are desired although it should be noted that these products already bear key motifs found in bioactive natural products.[23] These products (**6h** and **7i**) were obtained from furan **1a** with good productivities for the first step in their synthesis (for **6h**: 0.26–0.38 mmol min^{-1} and for **7i**: 0.29 mmol min^{-1}) and with high overall yields (50–62%). Alternatively, in entries j and k the products were derived through the combination of a second oxidation which introduced an extra degree of unsaturation and then reaction of the NAI intermediate with an internal nucleophile (appended as part of either R^1 or R^2). These products (**8j** and **9k**) were obtained from the corresponding furans **1a** and **1d** with high overall yields (49–66%). Unlike the two reaction modes described previously in Tables 1 and 2, there appeared to be no benefit to be gained in terms of the isolated yields on changing the positioning (horizontal to vertical) of the CFR Pyrex chamber for these reaction sequences, but improved conversion was observed for **1d** (95 vs 85%) even at higher flow rates (0.74 vs 0.54 mL min^{-1}). Changing the nebulizing gas from oxygen to air did not significantly impede the reactions (entries h and k). It is important to reiterate here that the products are attained after two very simple processes; substrate oxidation within the NebPhotOX followed by all remaining reactions in the collection vessel. The processes are operationally extremely simple and yet they oversee very dramatic alterations in functionality and increases in molecular complexity.

Overall, a number of different reaction sequences which all have very high overall yields and which target a broad range of privileged nitrogen-bearing scaffolds have been developed. The initial step in these sequences occurs in a continuous flow photoreactor and all the remaining operations take place in a single pot. The complete reaction sequences, which oversee dramatic increases in both molecular complexity and diversity, are operationally very simple to undertake. The continuous flow photoreactor irradiates a nebulized reaction solution and attains very high conversions and productivities for the key first step of the reaction bundles. Fixing the reactor's Pyrex chamber vertically, rather than angled horizontally, has been shown to increase conversions and isolated yields in some cases. Crucially, it has also been proven that changing the nebulizer gas from oxygen to air does not significantly affect the outcome with conversions only slightly diminished by this important adjustment. Simple green reagents and solvents are employed and

the initial substrates are readily accessible and easy to manipulate furans.

Acknowledgements

The research leading to these results has received funding from the European Research Council under the European Union's Seventh Framework Programme (FP7/2007-2013)/ERC grant agreement no. 277588. In addition, this project has received funding from the European Research Council (ERC) under the European Union's Horizon 2020 research and innovation programme (grant agreement No 779437). We thank Mr. Georgios Papadakis from the Electrical Workshop for help in assembling the electrical components of the photoreactor.

Conflict of Interest

The authors declare no conflict of interest.

Keywords: Aerosol · continuous flow reactor · *N*-acyl imminium · nebulizer · singlet oxygen

[1] J. B. Hendrickson, *J. Am. Chem. Soc.* **1975**, *97*, 5784–5800.
[2] a) T. Newhouse, P. S. Baran, R. W. Hoffmann, *Chem. Soc. Rev.* **2009**, *38*, 3010–3021; b) T. Gaich, P. S. Baran, *J. Org. Chem.* **2010**, *75*, 4657–4673.
[3] a) T. Montagnon, D. Kalaitzakis, M. Sofiadis, G. Vassilikogiannakis, *Org. Biomol. Chem.* **2016**, *14*, 8636–8640; b) T. Montagnon, D. Kalaitzakis, M. Triantafyllakis, M. Stratakis, G. Vassilikogiannakis, *Chem. Commun.* **2014**, *50*, 15480–15498; c) D. Kalaitzakis, M. Triantafyllakis, I. Alexopoulou, M. Sofiadis, G. Vassilikogiannakis, *Angew. Chem. Int. Ed.* **2014**, *53*, 13201–13205; *Angew. Chem.* **2014**, *126*, 13417–13421; d) D. Noutsias, I. Alexopoulou, T. Montagnon, G. Vassilikogiannakis, *Green Chem.* **2012**, *14*, 601–604.
[4] For a wide-ranging recent review of the intramolecular reactions of *N*-acyl imminium ions, see: P. Wu, T. E. Nielsen, *Chem. Rev.* **2017**, *117*, 7811–7856.
[5] For a two-part review of the intermolecular reactions of *N*-acyl imminium ions, see: a) A. Yazici, S. G. Pyne, *Synthesis* **2009**, *3*, 339–368; b) A. Yazici, S. G. Pyne, *Synthesis* **2009**, *4*, 513–541; and, for selected recent examples, see: c) D. Glavač, C. Zheng, I. Dokli, S.-L. You, M. Gredičak, *J. Org. Chem.* **2017**, *82*, 8752–8760; d) F. Fang, G. Hua, F. Shi, P. Li, *Org. Biomol. Chem.* **2015**, *13*, 4395–4398; e) Y.-C. Shi, S.-G. Wang, Q. Yin, S.-L. You, *Org. Chem. Front.* **2014**, *1*, 39–43.
[6] a) D. Kalaitzakis, M. Triantafyllakis, G. I. Ioannou, G. Vassilikogiannakis, *Angew. Chem. Int. Ed.* **2017**, *56*, 4020–4023; *Angew. Chem.* **2017**, *129*, 4078–4081; b) D. Kalaitzakis, M. Triantafyllakis, M. Sofiadis, D. Noutsias, G. Vassilikogiannakis, *Angew. Chem. Int. Ed.* **2016**, *55*, 4605–4609; *Angew. Chem.* **2016**, *128*, 4681–4685; c) D. Kalaitzakis, E. Antonatou, G. Vassilikogiannakis, *Chem. Commun.* **2014**, *50*, 400–402; d) D. Kalaitzakis, T. Montagnon, E. Antonatou, G. Vassilikogiannakis, *Org. Lett.* **2013**, *15*, 3714–3717; e) D. Kalaitzakis, T. Montagnon, E. Antonatou, N. Bardají, G. Vassilikogiannakis, *Chem. Eur. J.* **2013**, *19*, 10119–10123; f) D. Kalaitzakis, T. Montagnon, I. Alexopoulou, G. Vassilikogiannakis, *Angew. Chem. Int. Ed.* **2012**, *51*, 8868–8871; *Angew. Chem.* **2012**, *124*, 8998–9001.
[7] For the original basic CFR concept, see: a) G. I. Ioannou, T. Montagnon, D. Kalaitzakis, S. A. Pergantis, G. Vassilikogiannakis, *ChemPhotoChem* **2017**, *1*, 173–177; b) G. I. Ioannou, T. Montagnon, D. Kalaitzakis, S. A. Pergantis, G. Vassilikogiannakis, *Org. Biomol. Chem.* **2017**, *15*, 10151–10155.
[8] For a general CFR review, see: a) M. B. Plutschack, B. Pieber, K. Gilmore, P. H. Seeberger, *Chem. Rev.* **2017**, *117*, 11796–11893; For reviews of relevant CFR oxidations, see; b) A. Gavriilidis, A. Constantinou, K. Hellgardt, K. K. Hii, G. J. Hutchings, G. L. Brett, S. Kuhn, S. P. Marsden, *React. Chem. Eng.* **2016**, *1*, 595–612; c) H. P. L. Gemoets, Y. Su; M. Shang, V. Hessel, R. Luque, T. Noël, *Chem. Soc. Rev.* **2016**, *45*, 83–117; d) C. A. Hone, D. M. Roberge, C. O. Kappe, *ChemSusChem* **2017**, *10*, 32–41; For reviews of CFR photochemistry, see: e) Y. Su, N. J. W. Straathof, V. Hessel, T. Noël, *Chem. Eur. J.* **2014**, *20*, 10562–10589; f) D. Cambié, C. Bottecchia, N. J. W. Straathof, V. Hessel, T. Noël, *Chem. Rev.* **2016**, *116*, 10276–10341; g) K. Loubière, M. Oelgemöller, T. Aillet, O. Dechy-Cabaret, L. Prat, *Chem. Eng. Process.* **2016**, *104*, 120–132.
[9] A. A. Ghogare, A. Greer, *Chem. Rev.* **2016**, *116*, 9994–10034.
[10] For some representative examples and leading references, see: a) O. Shvydkiv, K. Jähnisch, N. Steinfeldt, A. Yavorskyy, M. Oelgemöller, *Catalysis Today*, **2018**, *308*, 102–118; b) C. Mendoza, N. Emmanuel, C. A. Páez, L. Dreesen, J.-C. Monbaliu, B. Heinrichs, *J. Photochem. Photobiol. A: Chem.* **2018**, *356*, 193–200; c) N. Emmanuel, C. Mendoza, M. Winter, C. Horn, A. Vizza, L. Dreesen, B. Heinrichs, J.-C. M. Monbaliu, *Org. Process Res. Dev.* **2017**, *21*, 1435–1438; d) A. Kouridaki, K. Huvaere, *React. Chem. Eng.* **2017**, *2*, 590–597; e) D. S. Lee, Z. Amara, C. A. Clark, Z. Xu, B. Kakimpa, H. P. Morvan, S. J. Pickering, M. Poliakoff, M. W. George, *Org. Process Res. Dev.* **2017**, *21*, 1042–1050; f) Y. Su, K. Kuijpers, V. Hessel, T. Noël, *React. Chem. Eng.* **2016**, *1*, 73–81; g) C. A. Clark, D. S. Lee, S. J. Pickering, M. Poliakoff, M. W. George *Org. Process Res. Dev.* **2016**, *20*, 1792–1798; h) A. Talla, B. Driessen, N. J. W. Straathof, L.-G. Milroy, L. Brunsveld, V. Hessel, T. Noël, *Adv. Synth. Catal.* **2015**, *357*, 2180–2186; i) D. B. Ushakov, K. Gilmore, D. Kopetzki, D. T. McQuade, P. H. Seeberger, *Angew. Chem. Int. Ed.* **2014**, *53*, 557–561; *Angew. Chem.* **2014**, *126*, 568–572; j) K. S. Elvira, R. C. R Wootton, N. M. Reis, M. R. Mackley, A. J. deMello, *ACS Sustainable Chem. Eng.* **2013**, *1*, 209–213; k) F. Lévesque, P. H. Seeberger, *Angew. Chem. Int. Ed.* **2012**, *51*, 1706–1709; *Angew. Chem.* **2012**, *124*, 1738–1741; l) A. A. Lapkin, V. M. Boddu, G. N. Aliev, B. Goller, S. Polisski, D. Kovalev, *Chem. Eng. J.* **2008**, *136*, 331–336.
[11] The Taylor flow concept is covered in detail alongside alternative gas-liquid phase mixing regimes in Refs. [8a, b, c, e, f].
[12] C. J. Mallia, I. R. Baxendale, *Org. Process Res. Dev.* **2016**, *20*, 327–360.
[13] For initial development of an FEP-coil continuous flow photoreactor, see: B. D. A. Hook, W. Dohle, P. R. Hirst, M. Pickworth, M. B. Berry, K. I. Booker-Milburn, *J. Org. Chem.* **2005**, *70*, 7558–7564.
[14] Comparisons of specific surface areas for different vessel types are presented in Ref. [12]. For example; 250 mL round bottom flasks, vertical tube reactors, and gas-liquid microchannel reactors have been assigned specific surface areas of 38, 100–2000 and 3400–18000 $m^2 m^{-3}$, respectively.
[15] Concomitant with the publication of our first prototype (Ref. [7a]), Zare and co-workers published a highly effective microdroplet spray reactor for achieving biphasic liquid-liquid reactions without the use of a phase transfer catalyst, see: X. Yan, H. Cheng, R. N. Zare, *Angew. Chem. Int. Ed.* **2017**, *56*, 3562–3565; *Angew. Chem.* **2017**, *129*, 3616–3619.
[16] Methanol is a preferred green solvent; see: F. M. Kerton in *Alternative Solvents for Green Chemistry*, RSC Publishing, Cambridge, **2009**, pp. 1–226.
[17] Full details of the prototype CFR set-up (including photographs) and all technical specifications are included in the Supporting Information.
[18] LED light tapes (neutral white light 3800–4200 K, 10 Wm^{-1}, 1050 Lmm^{-1}) were mounted onto a piece of plastic sheeting joined along its long edges to make a cylindrical jacket.
[19] J. Turconi, F. Griolet, R. Guevel, G. Oddon, R. Villa, A. Geatti, M. Hvala, K. Rossen, R. Göller, A. Burgard, *Org. Process Res. Dev.* **2014**, *18*, 417–422.
[20] For the batch synthesis, see; G. I. Ioannou, D. Kalaitzakis, G. Vassilikogiannakis, *Eur. J. Org. Chem.* **2016**, 3304–3306.
[21] Productivity for the photooxidation (mmol min^{-1}) = concentration × flow rate × conversion.
[22] a) D. Kalaitzakis, A. Kouridaki, D. Noutsias, T. Montagnon, G. Vassilikogiannakis, *Angew. Chem. Int. Ed.* **2015**, *54*, 6283–6287; *Angew. Chem.* **2015**, *127*, 6381–6385; b) D. Kalaitzakis, D. Noutsias, G. Vassilikogiannakis, *Org. Lett.* **2015**, *17*, 3596–3599.
[23] These motifs are ubiquitous, as leading references, see Refs. [3a] and [6b].

Manuscript received: March 13, 2018
Accepted Article published: April 15, 2018
Version of record online: May 2, 2018